Icarus **155**, 382–392 (2002)
doi:10.1006/icar.2001.6720, available online at http://www.idealibrary.com on IDEAL®

Evolution of CO on Titan

Ah-San Wong, Christopher G. Morgan, and Yuk L. Yung

Division of Geological and Planetary Sciences, California Institute of Technology, 150-21, Pasadena, California 91125
E-mail: asw@gps.caltech.edu

and

Tobias Owen

Institute for Astronomy, University of Hawaii, Honolulu, Hawaii 99822

Received May 11, 2001; revised July 12, 2001

The early evolution of Titan's atmosphere is expected to produce enrichment in the heavy isotopomers of CO, ^{13}CO and C^{18}O, relative to ^{12}C^{16}O. However, the original isotopic signatures may be altered by photochemical reactions. This paper explains why there is no isotopic enrichment in C in Titan's atmosphere, despite significant enrichment of heavy H, N, and O isotopes. We show that there is a rapid exchange of C atoms between the CH_4 and CO reservoirs, mediated by the reaction $^1CH_2 + {}^*CO \rightarrow {}^{1*}CH_2 + CO$, where *C is ^{13}C. Based on recent laboratory measurements, we estimate the rate coefficient for this reaction to be 3.2×10^{-12} cm^3 s^{-1} at the temperature appropriate for the upper atmosphere of Titan. We investigate the isotopic dilution of CO using the Caltech/JPL one-dimensional photochemical model of Titan. Our model suggests that the time constant for isotopic exchange through the above reaction is about 800 Myr, which is significantly shorter than the age of Titan, and therefore any original isotopic enhancement of ^{13}C in CO may have been diluted by the exchange process. In addition, a plausible model for the evolution history of CO on Titan after the initial escape is proposed.

Key Words: **Titan; atmosphere; evolution; composition.**

1. INTRODUCTION

In the first paper on the photochemistry of hydrocarbons on Titan, Strobel (1974) pointed out the fundamental difference between the stability of methane on Jupiter and that on Titan. On Jupiter CH_4 is destroyed in the upper atmosphere by photolysis and converted to higher hydrocarbons and hydrogen. The products are eventually transported to the lower atmosphere, where thermodynamic equilibrium at high temperature and pressure recycles the hydrocarbons and hydrogen back to CH_4. However, on Titan the destruction of CH_4 is irreversible. The higher hydrocarbons condense on the surface, and hydrogen escapes to space. To maintain the atmosphere in steady state, Strobel (1974) suggested that CH_4 must be replenished by outgassing from the crust, which is thought to be composed of CH_4 and NH_3 hydrates (Lewis 1971). Subsequent observations by *Voyager* and modeling largely confirmed the idea of the transient nature of Titan's atmosphere (see, for example, Yung *et al*. 1984). From the photochemical model of Yung *et al*. (1984), the column abundance and rate of destruction for CH_4 are 4.6×10^{24} cm^{-2} and 1.5×10^{10} cm^{-2} s^{-1}, respectively. Therefore the lifetime of CH_4 in the atmosphere is about 10 Myr, which is very short compared with the age of the Solar System, 4.6 Gyr. Yung *et al*. (1984) also extended Strobel's idea to N_2 and CO on Titan, and the relevant quantities are summarized in Table I. Their work concludes that over the age of the Solar System, N_2 is fairly stable, and CO is much less stable. In this work, we will revise the quantitative rate of change of CO in Table I. It should be emphasized that the destruction rates are based on extrapolation of present photochemical rates in the model. The model does not include alternative paths of evolution (see, for example, Lorenz *et al*. 1997) or what might have happened during the period close to the origin of the atmosphere (Atreya *et al*. 1978, Lunine *et al*. 1999, Lammer *et al*. 2000).

Pinto *et al*. (1986) pointed out that the relative abundances of the isotopomers of CH_4 could be used to constrain the evolutionary history of Titan's atmosphere. This idea is based on the fact that chemical destruction or escape to space differentiates among isotopomers, resulting in measurable isotopic fractionations. This idea can be applied to all other species, such as CO, N_2, or HCN. Figure 1 summarizes the isotopic measurements on Titan for hydrogen, carbon, nitrogen, and oxygen, plotted relative to the protosolar (for deuterium) or terrestrial values (for carbon, nitrogen, and oxygen). All D/H enhancements are inferred from measurements of CH_3D/CH_4 ratios, which are:

$$\mathrm{D/H} = 16.1^{+16.5}_{-8} \times 10^{-5}$$

from ground-based data (De Bergh *et al*. 1988),

$$15.0^{+14.0}_{-5.0} \times 10^{-5}$$

0019-1035/02 $35.00

TABLE I
Summary of Column Abundances, Destruction Rates, and Lifetimes of CH_4, N_2, and CO on Titan

	Column abundance (cm^{-2})	Destruction rate (cm^{-2} s^{-1})	Lifetime (years)
CH_4	4.59×10^{24}	1.5×10^{10}	9.7×10^{6}
N_2	2.30×10^{26}	2.8×10^{8}	2.6×10^{10}
CO	1.38×10^{22}	6.1×10^{5}	2.1×10^{9}

Note. From Yung *et al*. (1984).

from *Voyager* spectra (Coustenis *et al*. 1989), $7.75(\pm 2.25) \times 10^{-5}$ from Infrared Telescope Facility (IRTF) measurements at 8.7 μm wavelength (Orton 1992), and $9.5(\pm 2.5) \times 10^{-5}$ from the short wavelength spectrometer (SWS) onboard ESA's Infrared Space Observatory (ISO) (Coustenis and Taylor 1999). The protosolar value of D/H is $2.6(\pm 0.7) \times 10^{-5}$ (Geiss and Gloeckler 1998, Mahaffy *et al*. 1998), which is 25% of the CH_3D/CH_4 ratio. The $^{13}C/^{12}C$ measurements are: $H^{13}CN/H^{12}CN$ through Earth-based millimeter measurements at 88.63 GHz by Hidayat *et al*. (1997) and $^{12}C^{13}CH_6/^{12}C^{12}CH_6$ from 12-μm wavelength spectra measurements by Orton (1992). The terrestrial value for $^{13}C/^{12}C$ adopted here is 0.011 (Van Dishoeck *et al*. 1993). The $^{15}N/^{14}N$ enrichment is determined from Earth-based millimetric wavelength spectroscopic observations of $HC^{15}N/HC^{14}N$ and the ratio is found to be 4.5 times that of the Earth value (Hidayat and Marten 1998). For $^{18}O/^{16}O$ enhancement, Owen *et al*. (1999) report a preliminary value of $^{18}O/^{16}O$ about twice the terrestrial value of 2×10^{-3} in the detection of the (3–2) line of $C^{18}O$ at 329.33 GHz in the radio spectrum. Figure 1 clearly shows that on Titan there is enrichment in heavy isotopes of H, N, and O, but not in C.

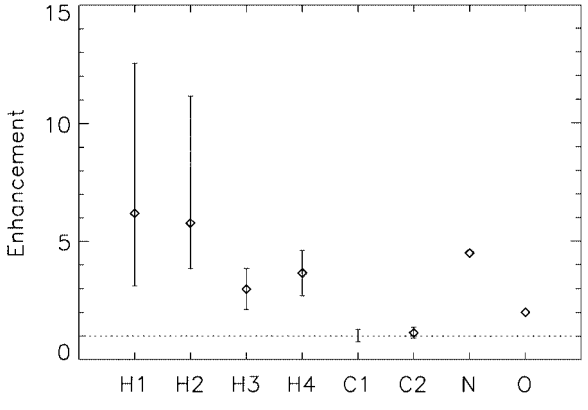

FIG. 1. Summary of the hydrogen, carbon, nitrogen, and oxygen isotopic measurements on Titan, plotted relative to the protosolar (for deuterium) or terrestrial value (for carbon, nitrogen, and oxygen). For D/H, H1 is from De Bergh *et al*. (1988), H2 is from Coustenis *et al*. (1989), H3 is from Orton (1992), and H4 is from Coustenis and Taylor (1999, pp. 76–97). For $^{13}C/^{12}C$, C1 is from HCN by Hidayat *et al*. (1997) and C2 is from C_2H_6 by Orton (1992). N is $^{15}N/^{14}N$ from Hidayat and Marten (1998). O is $^{18}O/^{16}O$ from CO by Owen *et al*. (1999). The protosolar value of D/H is $2.6(\pm 0.7) \times 10^{-5}$ (Geiss and Gloeckler 1998, Mahaffy *et al*. 1998). The terrestrial value for $^{13}C/^{12}C$ is 0.011 (Van Dishoeck *et al*. 1993); for $^{15}N/^{14}N$ it is 3.68×10^{-3} and for $^{18}O/^{16}O$ it is 2×10^{-3}.

According to Yung *et al*. (1984), about 17% of the original N_2 on Titan has been destroyed by escape to space and loss to the ground. However, on the basis of the isotopic data, Lunine *et al*. (1999) proposed that there was an early period of massive escape of atmospheric species. The driving force could have been the more active phase of the Sun in the early history of Titan (Pepin 1991, Kass and Yung 1995, Lammer *et al*. 2000). Like N_2, a large amount of CO could have been lost by escape from Titan in the past. We expect by analogy with N_2 that the heavy isotopomers of CO, ^{13}CO, and $C^{18}O$ would be enriched relative to $^{12}C^{16}O$. However, because of the source of new CH_4 from the interior of the satellite, carbon enrichment in CO could be diluted, if a chemical pathway exists for exchange between the carbon atoms in CH_4 and CO. This latter possibility is investigated in this paper using an updated version of the Caltech/JPL one-dimensional photochemical model of Titan.

The present work is primarily motivated by the curious isotopic fractionation of CO, as summarized in Fig. 1. According to Hidayat and co-workers (1997, 1998), the $^{13}CO/^{12}CO$ ratio is the same as $H^{13}CN/H^{12}CN$, which is close to the terrestrial value. However, the $C^{18}O/C^{16}O$ ratio is twice the terrestrial value (Owen *et al*. 1999). Why is there an enrichment in $C^{18}O$ but not in ^{13}CO? To address this question, we carry out a critical examination of the chemical kinetics relevant to CO on Titan, followed by modeling of the evolution of CO and its isotopomers. The methodology adopted in the evolution model is based on that of McElroy and Yung (1976).

2. KINETICS

The photochemical model adopted in this work is based on Yung *et al*. (1984) and Moses *et al*. (2000a). There are several important modifications of the kinetics, which are discussed in detail in this section. All reaction numbers refer to the reaction list of the complete Titan model. The reactions discussed in this paper are listed in Table II. The species $^1CH_2$ and $^3CH_2$ refer to the singlet (excited) and triplet (ground) state of the methylene radical, respectively. A schematic diagram showing the major reaction pathways and ultimate fate of the oxygen atom derived from meteoritic H_2O is shown in Fig. 2.

2.1. $OH + CH_3$

We examine three reaction channels for the reaction between OH and CH_3:

$$OH + CH_3 \rightarrow CO + 2H_2 \quad (1)$$

$$OH + CH_3 \rightarrow H_2O + {}^1CH_2 \quad (2)$$

$$OH + CH_3 \rightarrow HCOH + H_2. \quad (3)$$

TABLE II
Partial List of Reactions

No.	Reaction	Rate constant	Reference
R136	$C + H_2 + M \rightarrow {}^3CH_2 + M$	$k_0 = 7.00 \times 10^{-32}$ $k_\infty = 2.06 \times 10^{-11} \exp(-57/T)$	Moses *et al*. 2000a
R137	$C + C_2H_2 + M \rightarrow C_3H_2 + M$	$k_0 = 1.00 \times 10^{-31}$ $k_\infty = 2.10 \times 10^{-10}$	Moses *et al*. 2000a
R247	$H_2O + h\nu \rightarrow H + OH$	4.947×10^{-8}	Moses *et al*. 2000a
R248	$H_2O + h\nu \rightarrow 2H + O$	3.197×10^{-9}	Moses *et al*. 2000a
R250	$CO + h\nu \rightarrow C + O$	3.450×10^{-9}	Moses *et al*. 2000a
R251	$CO_2 + h\nu \rightarrow CO + O$	6.801×10^{-11}	Moses *et al*. 2000a
R253	$HCO + h\nu \rightarrow H + CO$	5.390×10^{-6}	Moses *et al*. 2000a
R254	$H_2CO + h\nu \rightarrow HCO + H$	4.307×10^{-7}	Moses *et al*. 2000a
R255	$H_2CO + h\nu \rightarrow H_2 + CO$	5.619×10^{-7}	Moses *et al*. 2000a
R269	$O + CH_3 \rightarrow H_2CO + H$	1.40×10^{-10}	Moses *et al*. 2000a
R280	$O + C_2H_4 \rightarrow H_2CCO + H_2$	$1.50 \times 10^{-19}\ T^{2.08}$	Moses *et al*. 2000a
R315	$OH + CH_3 \rightarrow H_2O + {}^1CH_2$	$1.0 \times 10^{-10}\ (T/300)^{-0.91} \exp(-275/T)$	Pereira *et al*. 1997
R320	$OH + C_2H_2 + M \rightarrow CH_3CO + M$	$k_0 = 2.6 \times 10^{-26}\ T^{-1.5}$ $k_\infty = 1.0 \times 10^{-17}\ T^{-2}$	Moses *et al*. 2000a
R329	$OH + CO \rightarrow CO_2 + H$	1.5×10^{-13}	Moses *et al*. 2000a
R344	$CO_2 + {}^3CH_2 \rightarrow CO + H_2CO$	2.8×10^{-15}	Darwin and Moore 1995
R407	$CH_3CO + H \rightarrow HCO + CH_3$	3.57×10^{-11}	Moses *et al*. 2000a
R410	$CH_3CO + CH_3 \rightarrow CO + C_2H_6$	4.9×10^{-11}	Moses *et al*. 2000a
R446	${}^1CH_2 + {}^*CO \rightarrow {}^{1*}CH_2 + CO$	3.2×10^{-12}	This work
R447	${}^1CH_2 + N_2 \rightarrow {}^3CH_2 + N_2$	$5.1 \times 10^{-13}\ T^{0.5}$	Ashfold *et al*. 1981
R448	$OH + CH_3 \rightarrow H_2CO + H_2$	$1.9 \times 10^{-14}\ (T/300)^{-0.12} \exp(209/T)$	Pereira *et al*. 1997

Note. Two-body rate constants and high-pressure limiting rate constants for three-body reactions (k_∞) are in units of $cm^3\ s^{-1}$. Low-pressure limiting rate constants for three-body reactions (k_0) are in units of $cm^6\ s^{-1}$. M represents any third body such as H_2. For photolysis reactions, the rate constants are the rate at 5×10^{-10} mbar.

Channel (1) is the major pathway to produce CO in Yung *et al*. (1984), where the rate constant k_1 (Yung) $= 6.7 \times 10^{-12}\ cm^3\ s^{-1}$. This is actually the overall reaction rate coefficient measured by Fenimore (1968). Although possible products may lead to the formation of CO, the products formed in his experiment and the branching ratios are unknown. Therefore channel (1) should no longer be included in our reaction list.

Channel (2) is the major channel for this reaction used by Moses *et al*. (2000a), where k_2 (Moses) $= 1.0 \times 10^{-12}\ cm^3\ s^{-1}$, taken from the experiment of Oser *et al*. (1992). We examined the work of the Oser group (Oser *et al*. 1992, Humpfer *et al*. 1995). They describe difficult and complicated experiments, and the analysis of the data is subject to many uncertainties. In particular, their reliance on the H versus D experiments is unreliable as there are many potential traps that they may or may not have encountered. For example, exchange of H_2O and HDO on the walls is common and depends on the history of past experiments. Even though they were generating plenty of D atoms from OD + OD, their model does not appear to include the exchange reaction $CH_3 + D \rightarrow CH_2D + H$, which is very fast at all pressures. Therefore, we no longer use their result for channel (2).

The reaction of OH with CH_3 is investigated by Deters *et al*. (1998). They observed singlet methylene directly in this reaction by laser magnetic resonance (LMR). They studied the rate coefficient and the product distribution of the reaction at room temperature in low pressures down to 0.7 mbar. The branching ratio for reaction channel (2) is 0.89 ± 0.09 at 1.33 mbar and 298 K. From their Fig. 7, extrapolating the falloff curve of the overall rate coefficient down to the low-pressure limit, we get k_{overall} (Deters) $= 3.3 \times 10^{-11}\ cm^3\ s^{-1}$. Using a branching ratio 0.89, k_2 (Deters) $= 3.0 \times 10^{-11}\ cm^3\ s^{-1}$ for channel (2).

The experimental measurements by Pereira *et al*. (1997) confirm the high-pressure limiting value for the overall reaction that several other groups have measured. They make a good case that channel (2) is approximately thermoneutral and not endothermic as suggested by Oser *et al*. (1992). Consequently they also favor channel (2) as the dominant reaction at the low pressures that are of interest to our modeling.

We use Pereira *et al*.'s (1997) calculations as a consistent set of rate coefficients for the different channels. Of the six possible product channels they studied, only channel (2) and (3) are significant at the low temperatures for which we are interested. From their Appendix B, using statistical mechanics, their results can be applied for temperatures $200 \leq T \leq 1200$ K. Extrapolation to 150 K should not add very much uncertainty to our model.

In our work, the reactions and the rate coefficients we adopted are

$$OH + CH_3 \rightarrow H_2O + {}^1CH_2, \qquad \text{(R315)}$$

$$k_{315} = 1.0 \times 10^{-10}(T/300)^{-0.91} \exp(-275/T)\ cm^3\ s^{-1},$$

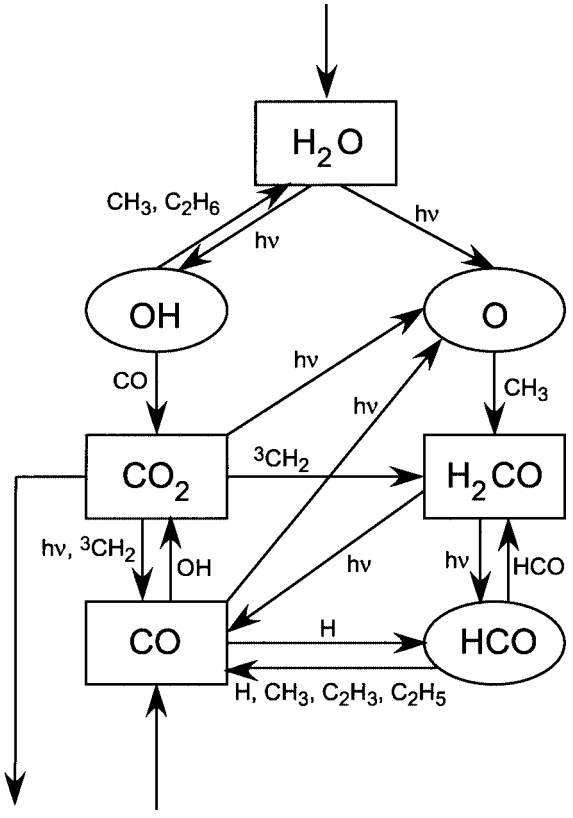

FIG. 2. Schematic diagram illustrating the important reaction pathways for oxygen species in our model. The symbol $h\nu$ corresponds to a solar ultraviolet photon. Radical species are outlined as ovals and stable molecules as rectangles.

$$\mathrm{OH} + \mathrm{CH_3} \rightarrow \mathrm{H_2CO} + \mathrm{H_2}, \qquad \text{(R448)}$$

$$k_{448} = 1.9 \times 10^{-14}\,(T/300)^{-0.12} \exp(209/T)\ \mathrm{cm^3\ s^{-1}}.$$

We note that the rate coefficient for R315 at 150 K is 3.0×10^{-11} cm^3 s^{-1}, which is consistent with the value obtained from Deters *et al.* (1998). For reaction R448, the rate coefficient at 150 K is 8.3×10^{-14} cm^3 s^{-1}. We assume that HCOH isomerizes to H_2CO rapidly.

2.2. $CO_2 + {}^3CH_2$

An important major pathway to produce CO is the reaction

$$\mathrm{CO_2} + {}^3\mathrm{CH_2} \rightarrow \mathrm{CO} + \mathrm{H_2CO}. \qquad \text{(R344)}$$

In Moses *et al.* (2000a), the rate coefficient for this reaction is taken from Laufer and Bass (1977) as 3.9×10^{-14} cm^3 s^{-1}. However, in a more recent work, Darwin and Moore (1995) measured the reactive removal rate of $^3CH_2$ with CO_2 directly and could not detect any reaction. Their upper limit for the rate coefficient of R344 is at least a factor of 3–5 lower than 1.4×10^{-14} cm^3 s^{-1}, a value much smaller than that from Laufer and Bass (1977). In our Titan model, we set the rate coefficient to be $k_{344} = 2.8 \times 10^{-15}$ cm^3 s^{-1}.

2.3. ${}^1CH_2 + N_2 \rightarrow {}^3CH_2 + N_2$

We add the quenching reaction (R447) of $^1CH_2$ by N_2,

$$\mathrm{{}^1CH_2} + \mathrm{N_2} \rightarrow \mathrm{{}^3CH_2} + \mathrm{N_2}. \qquad \text{(R447)}$$

Ashfold *et al.* (1981) measured the cross section for quenching of $^3CH_2$ by collisions with N_2 to be 1.1×10^{-16} cm^2. The temperature-dependent rate coefficient for quenching of $^1CH_2$ and N_2 is $k_{447} = 5.1 \times 10^{-13}\ T^{0.5}$ cm^3 s^{-1}. Note that Langford *et al.* (1983) reported a larger collisional cross section for $^1CH_2$ and N_2 than the one reported in Ashfold *et al.* (1981), but their experimental method measured the collisional cross section for removal of a specific rotational and vibrational state of $^1CH_2$ rather than the cross section for removal from the singlet electronic state.

2.4. Carbon Exchange Reaction

Carbon atom exchange has been observed between $^1CH_2$ and CO (Montague and Rowland 1971). The reaction rate for the exchange reaction (R446)

$$\mathrm{{}^1CH_2} + {}^*\mathrm{CO} \rightarrow \mathrm{{}^{1*}CH_2} + \mathrm{CO}, \qquad \text{(R446)}$$

where $^*C$ is ^{13}C, has a corresponding rate coefficient k_{446}. A reaction scheme for the exchange mechanism, which involves a ketene intermediary, is

$$\begin{aligned}
\mathrm{{}^1CH_2} + {}^*\mathrm{CO} &\xrightarrow{k_a} \mathrm{CH_2{}^*CO} \\
\mathrm{CH_2{}^*CO} &\xrightarrow{k_d} \mathrm{{}^1CH_2} + {}^*\mathrm{CO} \\
\mathrm{CH_2{}^*CO} &\xleftrightarrow{k_i} \mathrm{{}^*CH_2CO} \\
\mathrm{{}^*CH_2CO} &\xrightarrow{k_d} \mathrm{{}^{1*}CH_2} + \mathrm{CO},
\end{aligned}$$

where k_a is the rate coefficient for association of $^1CH_2$ and $^*CO$, k_d is the rate coefficient of ketene dissociation, and k_i is the rate coefficient for isomerization. The rate coefficients of dissociation and isomerization have been shown, within experimental error, to be the same for both ketene isotopomers (Lovejoy *et al.* 1991).

If steady-state concentrations are assumed for both ketene species, then the rate of carbon atom exchange between $^1CH_2$ and $^*CO$ is

$$\mathrm{Rate} = k_{446}\big[{}^1\mathrm{CH_2}\big]\big[{}^*\mathrm{CH_2}\big] = \frac{k_a k_i}{k_d + 2k_i}\big[{}^1\mathrm{CH_2}\big]\big[{}^*\mathrm{CH_2}\big].$$

The quantity $k_i/(k_d + 2k_i)$ is equal to the yield for carbon atom exchange (Y) for a given association of $^1CH_2$ and $^*CO$. The yield for carbon atom exchange between $^1CH_2$ and CO can be quantitatively estimated from the experimental work of the Moore group (Lovejoy *et al.* 1991, Lovejoy and Moore 1993). In their work, $CH_2{}^{13}CO$ was photodissociated and the appearance of

CO and ^{13}CO was monitored as a function of photolysis wavelength. During the ketene photolysis, the molecule is promoted to an excited singlet state. It then undergoes a radiationless transition to the ground-state singlet manifold. At that point, ketene can either transfer through intersystem crossing to the triplet manifold or undergo either isomerization or dissociation in the ground-state singlet manifold (Cui and Morokuma 1997). In the carbon exchange reaction (R446), the $^1CH_2$ and CO also form a ketene intermediary in the ground-state singlet manifold. Since both the ketene intermediary during carbon atom exchange and the ketene in the photolysis experiments undergo isomerization from the ground singlet state, the pathways for carbon exchange for the $^1CH_2 + CO$ reaction and the photodissociation reaction are the same. Therefore, the photodissociation studies of ketene are a suitable proxy for us to deduce the rate coefficients of the reaction scheme listed above.

The threshold for singlet CH_2*CO dissociation is 30,137 cm^{-1} (Chen *et al.* 1988, Lovejoy *et al.* 1991). The data of Lovejoy *et al.* (1991), taken between 30,137 and 32,000 cm^{-1}, are fit to a quadratic function (see Fig. 3). Since we are only interested in the order of magnitude of the exchange rate, we have greatly simplified the calculation by assuming that in the reaction of $^1CH_2$ and CO, only translational energy will provide the excess energy of the complex formation. More detailed calculations of the exchange rate, including the role of rotational and vibrational energy, are left for later study. If the quadratic function in Fig. 3 is convolved over the Boltzmann translational energy distribution, the following temperature-dependent yield for carbon atom exchange ($Y(T)$) can be calculated:

$$\frac{k_i}{(k_d + 2k_i)} = Y(T) = 0.100 - 1.11 \times 10^{-4}\, T + 8.0 \times 10^{-8}\, T^2.$$

At a temperature typical of the upper atmosphere of Titan, 200 K, the yield is $Y = 0.081$.

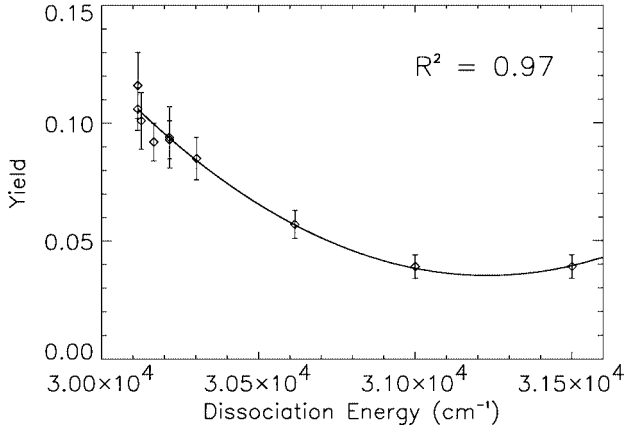

FIG. 3. The diamonds (with error bars) are the carbon atom exchange yields between $^1CH_2$ and CO, measured by Lovejoy *et al.* (1991) as a function of photodissociation energy. The solid line is the quadratic fit to the data (with $R^2 = 0.97$).

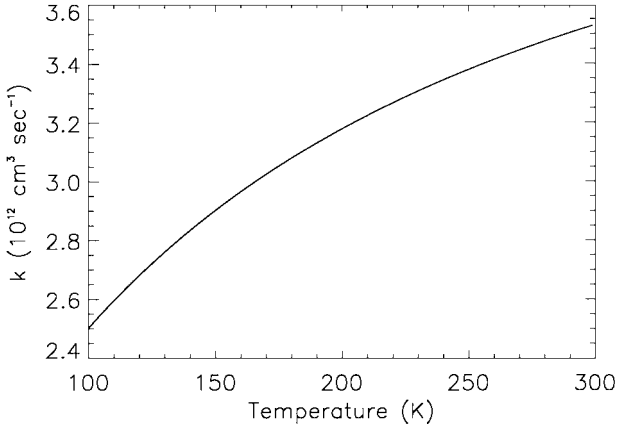

FIG. 4. The carbon exchange rate coefficient k_{446} between $^1CH_2$ and CO as a function of temperature.

The association rate coefficient of $^1CH_2$ and *CO, k_a, can be estimated using the reactive hard-sphere model, which states that the association rate coefficient is equal to the products of the total cross section for association (σ_a) between $^1CH_2$ and *CO and the average relative velocity (Steinfeld *et al.* 1989), or

$$k_a = \sigma_a \sqrt{\frac{8RT}{\pi M}},$$

where R is the ideal gas constant and M is the reduced mass of the system. Using σ_a rather than a simple collisional cross section takes into account that only inelastic collisions between $^1CH_2$ and CO lead to the formation of the ketene intermediary. Langford *et al.* (1983) have measured the cross section for these inelastic collisions to be 6.0×10^{-16} cm^2. Therefore, the temperature-dependent rate coefficient for carbon atom exchange between $^1CH_2$ and CO is

$$k_{446} = k_a\, Y(T) = 2.8 \times 10^{-13}\, T^{1/2} - 3.2 \times 10^{-16}\, T^{3/2} + 2.2 \times 10^{-19}\, T^{5/2} \text{ cm}^3 \text{ s}^{-1}.$$

A plot of the rate coefficient versus temperature is shown in Fig. 4. At 200 K, the above expression gives a rate coefficient of $k_{446} = 3.2 \times 10^{-12}$ cm^{-3} s^{-1}.

If this reaction is fast enough, the carbon atoms in CO will be exchanged with the carbon atoms in the CH_4 in the atmosphere, and *any original isotopic fractionation of carbon in CO can be diluted by this process over time*, assuming the presence of a major source/reservoir of CH_4, already required by the short lifetime of this species in the atmosphere.

2.5. *Dissociation of CO*

We now investigate other possible processes involved in isotopic exchange in CO. An important process is the dissociation

of CO into C and O via the following reactions R250:

$$\mathrm{CO} + h\nu \rightarrow \mathrm{C} + \mathrm{O} \quad \text{(R250a)}$$
$$\mathrm{CO} + e^- \rightarrow \mathrm{C} + \mathrm{O} + e^- \quad \text{(R250b)}$$
$$\mathrm{CO} + h\nu \rightarrow \mathrm{CO}^+ + e^- \quad \text{(R250c)}$$
$$\mathrm{CO}^+ + e^- \rightarrow \mathrm{C} + \mathrm{O}. \quad \text{(R250d)}$$

While some of the C and O atoms produced in the breakup processes can escape to space, for those C and O that remain in the atmosphere, their fates are quite different with respect to exchange with other reservoirs.

The most important reactions for O are insertions into CH_3 and C_2H_4 (Yung *et al*. 1984), such as

$$\mathrm{O} + \mathrm{CH_3} \rightarrow \mathrm{H_2CO} + \mathrm{H} \quad \text{(R269)}$$

followed by

$$\mathrm{H_2CO} + h\nu \rightarrow \mathrm{H_2} + \mathrm{CO} \quad \text{(R255)}$$
$$\mathrm{H_2CO} + h\nu \rightarrow \mathrm{HCO} + \mathrm{H} \quad \text{(R254)}$$
$$\mathrm{HCO} + h\nu \rightarrow \mathrm{H} + \mathrm{CO}. \quad \text{(R253)}$$

Although four different product channels result from the reaction between O and C_2H_4,

$$\mathrm{O} + \mathrm{C_2H_4} \rightarrow \text{products}, \quad \text{(R277–280)}$$

they all eventually produce a CO molecule via reactions similar to R253–255. In the re-formation of the CO molecule, the O atom is derived originally from CO, because CO is the principal atmospheric reservoir of oxygen. *Thus the isotopic signature of O in CO will be preserved.*

We make a similar inquiry into the fate of the C atom produced in the CO breakup (R250). The C atom in the re-formed CO comes from CH_3 and C_2H_4, which in turn are derived from CH_4 photolysis. The primary reactions removing C atoms are the following (Moses *et al*. 2000a):

$$\mathrm{C} + \mathrm{H_2} + M \rightarrow {}^3\mathrm{CH_2} + M \quad \text{(R136)}$$
$$\mathrm{C} + \mathrm{C_2H_2} + M \rightarrow \mathrm{C_3H_2} + M, \quad \text{(R137)}$$

where M represents any third body. The ultimate fate of the CH_2 and C_3H_2 radicals on Titan is to form heavier hydrocarbons that condense on the surface and are *permanently sequestered in the ground reservoir* (Yung *et al*. 1984). *This process does not preserve the isotopic signature of C in CO.*

If the rate for the CO dissociation reaction R250 is slow compared with the age of the Solar System, then this process is unimportant in altering the isotopic fractionation of CO. The reaction rate is calculated and shown in the next section.

3. MODEL AND RESULTS

We updated the H_2O influx at the upper boundary from 6.1×10^5 (Yung *et al*. 1984) to 1.5×10^6 cm^{-2} s^{-1} to agree with observations (Coustenis *et al*. 1998). This updated flux is within the predicted range of (0.8–2.8) $\times 10^6$ cm^{-2} s^{-1} from Moses *et al*. (2000b).

In our standard model, the CO mixing ratio is set to 5.2×10^{-5}, which is consistent with the measurements of Lutz *et al*. (1983), Muhleman *et al*. (1984), and Gurwell and Muhleman (1995, 2000). However, Marten *et al*. (1988), Noll *et al*. (1996), and Hidayat *et al*. (1997) found significantly lower values. Since the chemical lifetime of CO on Titan is very long (on the order of 10^9 years) compared with atmospheric transport time scales, we expect CO to be well mixed in the atmosphere and there should be little change from year to year. In the unlikely event that CO is not well mixed in the atmosphere, we must conclude that there is an unknown reaction that destroys CO on Titan. Thus the discrepancies between the observations are puzzling and must be resolved by future measurements.

From the model we can calculate the time constants for carbon exchange reaction R446 and CO dissociation reaction R250. The reaction rates for these two reactions are plotted in Fig. 5. The column-integrated rates for R446 and R250 are 5.68×10^5 and 8.15×10^4 cm^{-2} s^{-1}, respectively. Since the column abundance of CO in the model is 1.42×10^{22} cm^{-2}, we get an exchange time constant of 792 Myr and a time constant for CO dissociation of 5.52 Gyr. The exchange reaction time constant is short compared with the age of the Solar System, which implies that the carbon atoms in CO will be exchanged with the carbon atoms in the atmospheric methane many times, and the original isotopic fractionation of carbon in CO can be diluted over time. On the other hand, the CO dissociation reaction time constant is long, which suggests that the process of CO dissociation is less important in the carbon exchange scheme and will not alter the isotopic signature of CO.

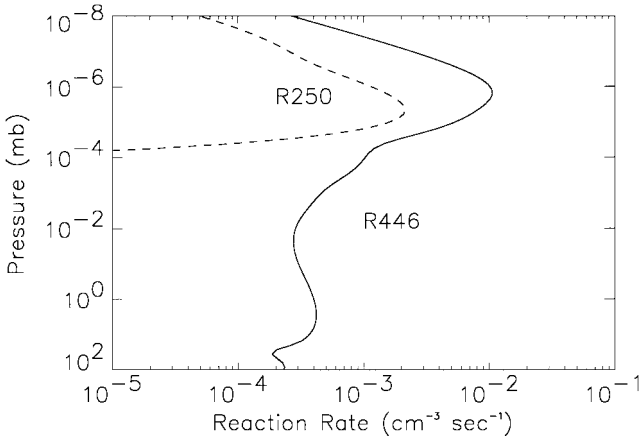

FIG. 5. Reaction rates for carbon exchange (R446) $^1\mathrm{CH_2} + {}^*\mathrm{CO} \rightarrow {}^{1*}\mathrm{CH_2} + \mathrm{CO}$ and CO dissociation (R250) $\mathrm{CO} \rightarrow \mathrm{C} + \mathrm{O}$.

With the update of the kinetics, the dominant CO production pathways are (in decreasing order of importance):

	$H_2O + h\nu \rightarrow H + OH$	(R247)
	$OH + CO \rightarrow CO_2 + H$	(R329)
	$CO_2 + {}^3CH_2 \rightarrow CO + H_2CO$	(R344)*
	$H_2CO + h\nu \rightarrow H_2 + CO$	(R255)
Net:	$H_2O + {}^3CH_2 \rightarrow CO + H_2 + 2H$	(Scheme 1)

and

	$H_2O + h\nu \rightarrow 2H + O$	(R248)*
	$O + CH_3 \rightarrow H_2CO + H$	(R269)
	$H_2CO + h\nu \rightarrow H_2 + CO$	(R255)
Net:	$H_2O + CH_3 \rightarrow CO + H_2 + 3H$	(Scheme 2)

and

	$H_2O + h\nu \rightarrow H + OH$	(R247)
	$OH + C_2H_2 \rightarrow CH_3CO$	(R320)
	$CH_3CO + CH_3 \rightarrow CO + C_2H_6$	(R410)*
Net:	$H_2O + C_2H_2 + CH_3 \rightarrow CO + C_2H_6 + H$	(Scheme 3)

and

	$H_2O + h\nu \rightarrow H + OH$	(R247)
	$OH + C_2H_2 \rightarrow CH_3CO$	(R320)
	$CH_3CO + H \rightarrow HCO + CH_3$	(R407)*
	HCO + hydrocarbons $\rightarrow$ CO + hydrocarbons	(R345–352)
Net:	$H_2O + C_2H_2$ + hydrocarbons $\rightarrow$ CO + hydrocarbons	(Scheme 4).

The limiting step for each scheme is labeled with an asterisk. Figure 2 shows the most important reaction pathways for oxygen species on Titan.

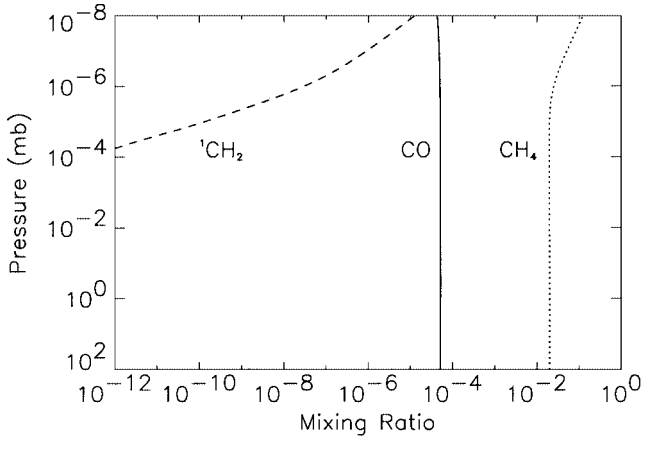

FIG. 6. Mixing ratios for CO, $^1CH_2$, and CH_4 in the standard Titan model.

TABLE III
Comparison of Model Results

	CO mixing ratio	CO upward flux (cm^{-2} s^{-1})	CO influx (cm^{-2} s^{-1})	H_2O influx (cm^{-2} s^{-1})
Yung *et al.* 1984	1.8×10^{-4}	0	8.8×10^{4}	6.1×10^{5}
Lara *et al.* 1996, 1998	5.0×10^{-5}	8.3×10^{5}	0	3.0×10^{6}
Lara *et al.* 1996, 1998 (equilibrium)	1.0×10^{-5}	0	0	3.0×10^{6}
Lara *et al.* 1996, 1998 (alternative)	5.0×10^{-5}	0	1.6×10^{6}	3.0×10^{6}
This work (standard)	5.2×10^{-5}	1.1×10^{6}	0	1.5×10^{6}
This work (equilibrium)	1.8×10^{-6}	0	0	1.5×10^{6}

The mixing ratios for $^1CH_2$, CH_4, and CO in our model are shown in Fig. 6. The values for $^1CH_2$ and CH_4 are not significantly different from those reported in the models of Yung *et al.* (1984) and Lara *et al.* (1996). Table III summarizes the results from different models.

The production rate of CO is much smaller than the loss rate. The CO mixing ratio of 5.2×10^{-5} is achieved through an upward flux of CO of about 1.1×10^{6} cm^{-2} s^{-1} from the surface. This can be compared to the model of Lara *et al.* (1996, 1998), where an upward flux of 8.3×10^{5} cm^{-2} s^{-1} CO is needed to maintain the conservation of O atoms and account for the mixing ratio of 5×10^{-5}. The influx of water in Lara *et al.* (1996, 1998) is about twice that in our standard model. They also proposed an alternative model in which, instead of an upward flux of CO from the surface, an influx of CO of 1.6×10^{6} cm^{-2} s^{-1} from meteoroids is required to reproduce the desired CO mixing ratio.

For CO to be in equilibrium and allow no external and/or internal source of CO to be supplied to the atmosphere, our model shows that the CO mixing ratio must be 1.8×10^{-6}, only 3% of the observed value. In a similar fashion, the steady-state CO mixing ratio found in Yung *et al.* (1984) is 100 times greater than our value, because of the inclusion of a fast CO production channel in their model (see earlier in this section). The steady-state CO mixing ratio found in Lara *et al.* (1996) is 5.6 times greater than ours, and we note the greater amount of water influx in their model.

4. EVOLUTION MODEL OF CO ISOTOPES

Since the water in meteorites is the major incoming source of oxygen on Titan, our model shows that the water influx is not large enough to sustain the observed amount of CO in the atmosphere. There are several possible explanations: (1) there is a continuous supply of CO from the interior on Titan (Dubouloz *et al.* 1989); (2) CO is directly injected into the atmosphere from incoming meteorites; (3) the amount of CO in the atmosphere is gradually decreasing; or (4) a combination of the above cases is in effect. We have discussed cases (1) and (2) in the previous section.

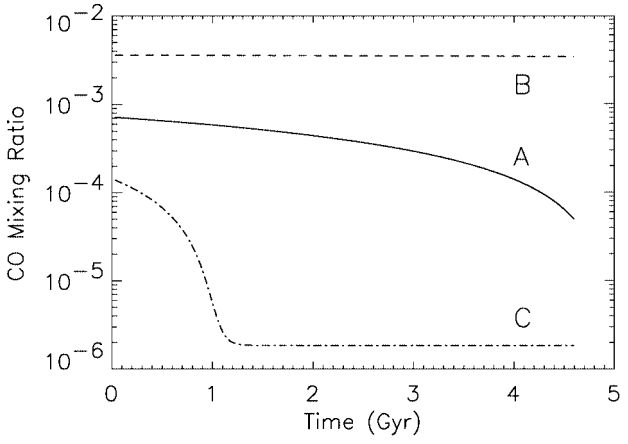

FIG. 7. Mixing ratio for CO as a function of time. Model A produces a mixing ratio of 5.2×10^{-5}, which is consistent with observation (Gurwell and Muhleman 2000), at present time (4.6 Gyr). Models B and C show the evolution with initial CO concentration 5 and 0.2 times of the initial value in the solid line, respectively.

For case (3), we can calculate the evolution history of CO in the atmosphere over time. With neither an external nor an internal supply of CO, to reach the CO mixing ratio of the present day, the CO mixing ratio after the initial escape stage at 4.6 Gyr ago would have to be 7.2×10^{-4}, 14 times more than the observed value of today. This is labeled model A. We have also calculated the evolution of CO with 5 times and 0.2 times the initial CO concentrations. For models B and C, the initial CO concentrations are 3.6×10^{-3} and 1.44×10^{-4}, respectively. Figure 7 shows the calculated mixing ratios as a function of time for the three models. The amount of CO lost over 4.6×10^9 years for models A, B, and C are 93.1, 5.3, and 98.7%, respectively. In model C, the CO abundance reaches a state of equilibrium and the final mixing ratio is 1.8×10^{-6}.

The evolution paths of the isotopomers of CO, ^{13}CO, and C^{18}O are different from ^{12}C^{16}O, and therefore the initial isotopic ratios in CO will be altered over time. To calculate the change of the isotopomers of CO, we need to determine the production rate $P(t)$, loss rate $L(t)$, and carbon atom exchange rate $E(t)$ for each isotopomer.

The production rate of each CO isotopomer is directly proportional to the ratio of the corresponding isotopes in the atmosphere. The destruction of CO occurs mainly through the reaction with OH:

$$\mathrm{OH} + \mathrm{CO} \rightarrow \mathrm{CO_2} + \mathrm{H}. \qquad \text{(R329)}$$

Since R329 is the major destruction route of CO, the loss rate of CO can be estimated as the column rate, or the vertically integrated chemical reaction rate, of R329. The reaction rate for R329 is slightly different for different isotopomers of CO due to mass-independent fractionation of the reaction. Let $^{12}k = k_{329}$, and let ^{13}k and ^{18}k be the overall rate coefficients for the system CO + OH for the isotopomers ^{13}CO and C^{18}O, respectively. From the work of Röckmann *et al.* (1998), by taking the low-pressure limit, we obtain the ratios $^{13}k/^{12}k = 1.005$ and $^{18}k/^{12}k = 1.011$.

To calculate the carbon atom exchange rate for ^{13}CO, consider the exchange reactions R446 and its backward reaction R446a,

$$^1\mathrm{CH_2} + {}^*\mathrm{CO} \rightarrow {}^{1*}\mathrm{CH_2} + \mathrm{CO} \qquad \text{(R446)}$$

$$^{1*}\mathrm{CH_2} + \mathrm{CO} \rightarrow {}^1\mathrm{CH_2} + {}^*\mathrm{CO}. \qquad \text{(R446a)}$$

If k_{446} and k_{446a} are the rate coefficients of these two reactions, then the rate of change in the concentration of *CO from the contribution of these two reactions is

$$\frac{d[{}^*\mathrm{CO}]}{dt} = -k_{446}[{}^1\mathrm{CH_2}][{}^*\mathrm{CO}] + k_{446a}[{}^{1*}\mathrm{CH_2}][\mathrm{CO}].$$

Since $k_{446} = k_{446a}$, the above expression can be reduced to

$$\frac{d[{}^*\mathrm{CO}]}{dt} = k_{446}[{}^1\mathrm{CH_2}]\left(\frac{[{}^{1*}\mathrm{CH_2}]}{[{}^1\mathrm{CH_2}]}[\mathrm{CO}] - [{}^*\mathrm{CO}]\right).$$

Letting the time constant of reaction R446 be $\tau_{ex} = (k_{446}[^1\mathrm{CH_2}])^{-1}$, we have

$$E(t) = \frac{d[{}^*\mathrm{CO}]}{dt} = \left(\frac{[{}^{1*}\mathrm{CH_2}]}{[{}^1\mathrm{CH_2}]}[\mathrm{CO}] - [{}^*\mathrm{CO}]\right)\tau_{ex}^{-1}.$$

The theory of isotopic enrichment in a planetary atmosphere due to photochemical processes has been worked out by McElroy and Yung (1976), whose methodology and notation we follow. Let $N_{12}(t)$, $N_{13}(t)$, and $N_{18}(t)$ be the total column abundance of ^{12}C^{16}O, ^{13}CO, and C^{18}O, respectively, on Titan at time t. The evolution of $N_{12}(t)$ is given by

$$\frac{dN_{12}(t)}{dt} = P_{12}(t) - L_{12}(t),$$

where time t is defined so that $t = 0$ refers to the time of formation of Titan and $t = 4.6 \times 10^9$ years corresponds to the present and $P_{12}(t)$ and $L_{12}(t)$ are the production rate and loss rate, respectively, of ^{12}C^{16}O from the evolution model.

Similarly, the evolution of ^{13}CO, in terms of $N_{13}(t)$, is given by

$$\frac{dN_{13}(t)}{dt} = P_{13}(t) - L_{13}(t) + E_{13}(t),$$

where $P_{13}(t)$, $L_{13}(t)$, and $E_{13}(t)$ are the production rate, loss rate, and exchange rate, respectively, of ^{13}CO. Here

$$P_{13}(t) = P_{12}(t)\left(\frac{^{13}\mathrm{C}}{^{12}\mathrm{C}}\right)_{\mathrm{CH_4}}$$

$$L_{13}(t) = L_{12}(t)\frac{^{13}k}{^{12}k}\frac{N_{13}(t)}{N_{12}(t)}$$

$$E_{13}(t) = \left(\frac{[^{13(1)}CH_2]}{[^{12(1)}CH_2]} N_{12}(t) - N_{13}(t) \right) \tau_{ex}^{-1}$$

and $[^{13(1)}CH_2]/[^{12(1)}CH_2] = 0.011$ (Van Dishoeck *et al*. 1993), where $\tau_{ex} = 7.92 \times 10^8$ years is the time constant for the exchange reaction calculated in the previous section.

For $C^{18}O$, the evolution of $N_{18}(t)$ is given by

$$\frac{dN_{18}(t)}{dt} = P_{18}(t) - L_{18}(t),$$

where the production and loss rates are

$$P_{18}(t) = P_{12}(t) \left(\frac{^{18}O}{^{16}O} \right)_{H_2O}$$

$$L_{18}(t) = L_{12}(t) \frac{^{18}k}{^{12}k} \frac{N_{18}(t)}{N_{12}(t)}.$$

We solve this set of equations by using the observed present value of $N_{12}(4.6 \times 10^9 \text{ years}) = 5.2 \times 10^{-5}$ and integrating the equations backward to $t = 0$ to obtain $N_{12}(t)$ and consequently $N_{13}(t)$ and $N_{18}(t)$. This gives us the enrichment factors of ^{13}CO to $^{12}C^{16}O$ and $C^{18}O$ to $^{12}C^{16}O$ as a function of time.

The result for model A is plotted in Fig. 8. We assume an initial enhancement of 3.23 for $C^{18}O/^{12}C^{16}O$ in order for the enhancement to reach the observed value (twice the terrestrial value) at present day. We set the initial enhancement for $^{13}CO/^{12}C^{16}O$ to be the same for the purpose of comparison. It is clear that if initially both heavy isotopomers of CO are enriched, through atmospheric evolution, ^{13}CO enrichment will dilute to close to unity (1.097), but $C^{18}O$ enrichment will dilute at a much slower rate. The results for models B and C are shown in Fig. 9. In both models, ^{13}CO is diluted rapidly to unity (1.105 and 1.095) because of the exchange of carbon atoms with the CH_4 reservoir in the atmosphere. The dilution of $C^{18}O$ is more gradual, especially in model B. Note that in model C, when equilibrium is reached, the $C^{18}O$ enrichment is close to the terrestrial value (0.989).

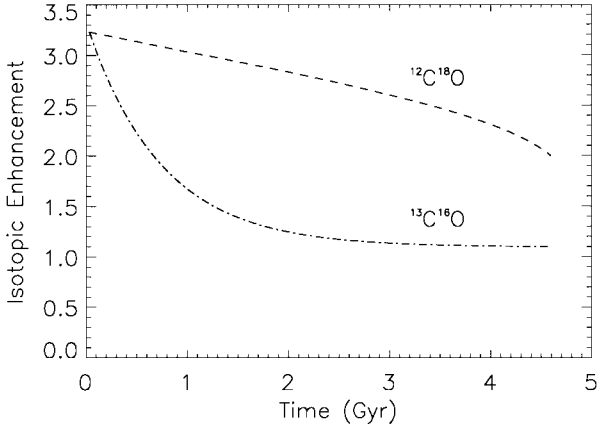

FIG. 8. Evolution of enrichment factors of $^{13}CO/^{12}C^{16}O$ and $C^{18}O/^{12}C^{16}O$ for model A, assuming an enrichment of 3.23 to the terrestrial value at time 0. The dashed line represents the enrichment of $C^{18}O$, and the dash-dot-dash line represents the enrichment of $C^{18}O$.

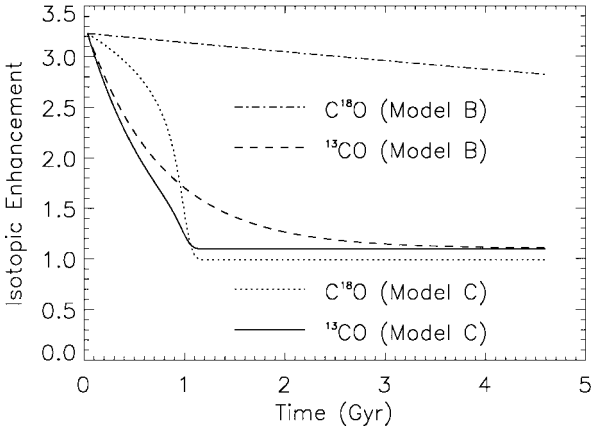

FIG. 9. Evolution of enrichment factors of ^{13}CO and $C^{18}O$ with respect to $^{12}C^{16}O$ for models B and C, assuming an enrichment of 3.23 to the terrestrial value at time 0.

5. CONCLUSION

Our study of the evolutionary history of CO on Titan has four implications: (1) there is evidence for massive loss of CO during Titan's early history, resulting in the enrichment of the isotopomers of CO except for ^{13}CO; (2) there has been a gradual decline in the concentration of CO in the atmosphere from about 14 times the present value to the present value; (3) as a result of an exchange reaction for carbon atoms, it is not possible to preserve the isotopic signature of ^{13}CO for longer than 800 Myr; and (4) the isotopic signatures of ^{17}O and ^{18}O isotopomers of CO are not diluted over the age of the Solar System. Our model presents a plausible but not unique interpretation of the known observations of Titan. To further our understanding of the evolutionary history of CO on Titan, it is most important to (1) resolve the differences in the measurements of CO abundance; (2) measure the isotopic fractionation of all three isotopomers, ^{13}CO, $C^{17}O$, and $C^{18}O$; and (3) measure the isotopic fractionation of all three isotopomers of CO on Saturn, where the source is exogenic, for comparison with Titan.

New laboratory measurements are needed to remove the uncertainties in the photochemistry and chemical kinetics of key reactions identified in our model. These include the branching ratio producing $^1CH_2$ in the UV photolysis of CH_4 and the products and branching ratio of the reaction of OH with CH_3.

ACKNOWLEDGMENTS

We thank F. S. Rowland for an illuminating discussion of the $^1CH_2$ and CO reaction and W. B. DeMore and K. Bayes for valuable advice on the kinetics of hydrocarbons and CO. We thank Nicolas Biver for carrying out the observations of Titan with the JCMT and J. I. Moses for providing the code on which the Titan model is based. M. Allen provided critical inputs to a preliminary version

of the paper, resulting in the present paper. We thank M. A. Gurwell and M. F. Gerstell for comments and suggestions. This research was supported in part by NAG5-6263 and the *Cassini* Project. C.G.M. thanks the National Research Council for an NRC Postdoctoral Fellowship.

REFERENCES

Ashfold, M. N. R., M. A. Fullstone, G. Hancock, and G. W. Ketley 1981. Singlet methylene kinetics: Direct measurements of removal rates of $\tilde{a}^1A_1$ and $\tilde{b}^1B_1$ CH_2 and CD_2. *Chem. Phys.* **55**, 245–257.

Atreya, S. K., T. M. Donahue, and W. R. Kuhn 1978. Evolution of a nitrogen atmosphere on Titan. *Science* **201**, 611–613.

Chen, I. C., W. H. Green, and C. B. Moore 1988. Bond breaking without barriers—Photofragmentation of ketene at the singlet threshold. *J. Chem. Phys.* **89**, 314–328.

Coustenis, A., and F. Taylor 1999. *Titan: The Earth-like Moon*. pp. 96–97. World Scientific, Singapore.

Coustenis, A., B. Bézard, and D. Gautier 1989. Titan atmosphere from Voyager infrared observations. II. The CH_3D abundance and D/H ratio from the 900–1200 cm^{-1} spectral region. *Icarus* **82**, 67–80.

Coustenis, A., A. Salama, E. Lellouch, Th. Encrenaz, G. L. Bjoraker, R. E. Samuelson, Th. de Graauw, H. Feuchtgruber, and M. F. Kessler 1998. Evidence for water vapor in Titan's atmosphere from ISO/SWS data. *Astron. Astrophys.* **336**, L85–L89.

Cui, Q., and K. Morokuma 1997. Ab initio study of nonadiabatic interactions in the photodissociation of ketene. *J. Chem. Phys.* **107**, 4951–4959.

Darwin, D. C., and C. B. Moore 1995. Reaction-rate constants (295 K) for ($^3CH_2$)–C-3 with H_2S, SO_2, and NO_2—Upper-bounds for rate constants with less reactive partners. *J. Phys. Chem.* **99**, 13467–13470.

de Bergh, C., B. L. Lutz, T. Owen, and J. Chauville 1988. Monodeuterated methane in the outer Solar System. III. Its abundance on Titan. *Astrophys. J.* **329**, 951–955.

Deters, R., M. Otting, H. G. Wagner, F. Temps, B. László, S. Dóbé, and T. Bérces 1998. A direct investigation of the reaction $CH_3 + OH$: Overall rate constant and CH_2 formation at $T = 298$ K. *Ber. Bunsen-Ges. Phys. Chem.* **102**, 58–72.

Dubouloz, N., F. Raulin, E. Lellouch, and D. Gautier 1989. Titan hypothesized ocean properties: The influence of surface temperature and atmospheric composition uncertainties. *Icarus* **82**, 81–96.

Fenimore, C. P. 1968. Destruction of methane in water gas by reaction of CH_3 with OH radicals. In *12th Symposium (International) on Combustion* (Eds.), pp. 463–467. Combustion Institute, Pittsburgh.

Geiss, J., and J. Gloeckler 1998. Abundances of deuterium and helium 3 in the protosolar cloud from solar wind measurements. *Space Sci. Rev.* **84**, 239–250.

Gurwell, M. A., and D. O. Muhleman 1995. CO on Titan: Evidence for a well-mixed vertical profile. *Icarus* **117**, 375–382.

Gurwell, M. A., and D. O. Muhleman 2000. CO on Titan: More evidence for a well-mixed vertical profile. *Icarus* **145**, 653–656.

Hidayat, T., and A. Marten 1998. Evidence for a strong $^{15}N/^{14}N$ enrichment in Titan's atmosphere from millimeter observations. *Ann. Geophys.* **16** (Suppl. III), C998 (abstract).

Hidayat, T., A. Marten, B. Bézard, D. Gautier, T. Owen, H. E. Matthews, and G. Paubert 1997. Millimeter and submillimeter heterodyne observations of Titan: Retrieval of the vertical profile of HCN and the $^{12}C/^{13}C$ ratio. *Icarus* **126**, 170–182.

Humpfer, R., H. Oser, and H. H. Grotheer 1995. Formation of $HCOH + H_2$ through the reaction $CH_3 + OH$; experimental evidence for a hitherto undetected product channel. *Int. J. Chem. Kinet.* **27**, 577–595.

Kass, D. M., and Y. L. Yung 1995. Loss of atmosphere from Mars due to solar wind-induced sputtering. *Science* **268**, 697–699.

Lammer, H., W. Stumptner, G. J. Molina-Cuberos, S. J. Bauer, and T. Owen 2000. Nitrogen isotope fractionation and its consequence for Titan's atmospheric evolution. *Planet. Space Sci.* **48**, 529–543.

Langford, A. O., H. Petek, and C. B. Moore 1983. Collisional removal of $CH_2(^1A_1)$—Absolute rate constants for atomic and molecular collisional partners at 295 K . *J. Chem. Phys.* **78**, 6650–6659.

Lara, L. M., E. Lellouch, J. J. López-Moreno, and R. Rodrigo 1996. Vertical distribution of Titan's atmospheric neutral constituents. *J. Geophys. Res.* **101**, 23261–23283.

Lara, L. M., E. Lellouch, J. J. Lopez–Moreno, and R. Rodrigo 1998. Correction to "Vertical distribution of Titan's atmospheric neutral constituents." *J. Geophys. Res.* **103**, 25775–25775.

Laufer, A. H., and A. M. Bass 1977. Reaction between triplet methylene and CO_2: Rate constant determination. *Chem. Phys. Lett.* **46**, 151–155.

Lewis, J. 1971. Satellites of the outer planets: Their physical and chemical nature. *Icarus* **15**, 174–185.

Lorenz, R. D., C. P McKay, and J. I. Lunine 1997. Photochemically driven collapse of Titan's atmosphere. *Science* **275**, 642–644.

Lovejoy, E. R., and C. B. Moore 1993. Structures in the energy-dependence of the rate-constant for ketene isomerization. *J. Chem. Phys.* **98**, 7846–7854.

Lovejoy, E. R., S. K. Kim, R. A. Alvarez, and C. B. Moore 1991. Kinetics of intramolecular carbon-atom exchange in ketene. *J. Chem. Phys.* **95**, 4081–4093.

Lunine, J. I., Y. L. Yung, and R. D. Lorenz 1999. On the volatile inventory of Titan from isotopic abundances in nitrogen and methane. *Planet. Space Sci.* **47**, 1291–1303.

Lutz, B. L., C. de Bergh, and T. Owen 1983. Titan: Discovery of carbon monoxide in its atmosphere. *Science* **220**, 1374–1375.

Mahaffy, P. R., T. M. Donahue, S. K. Atreya, T. C. Owen, and H. B. Niemann 1998. Galileo probe measurements of D/H and $^3He/^4He$ in Jupiter's atmosphere. *Space Sci. Rev.* **84**, 251–263.

Marten, A., D. Gautier, L. Tanguy, A. Lecacheux, C. Rosolen, and G. Paubert 1988. Abundance of carbon monoxide in the stratosphere of Titan from millimeter heterodyne observations. *Icarus* **76**, 558–562.

McElroy, M. B., and Y. L. Yung 1976. Oxygen isotopes in the martian atmosphere: Implications for the evolution of volatiles. *Planet. Space Sci.* **24**, 1107–1113.

Montague, D. C., and F. S. Rowland 1971. Oxirene intermediate in the reaction of singlet methylene with carbon monoxide. *J. Am. Chem. Soc.* **93**, 5381–5387.

Moses, J. I., B. Bézard, E. Lellouch, G. R. Gladstone, H. Feuchtgruber, and M. Allen 2000a. Photochemistry of Saturn's atmosphere. I. Hydrocarbon chemistry and comparisons with ISO observations. *Icarus* **143**, 244–298.

Moses, J. I., E. Lellouch, B. Bézard, G. R. Gladstone, H. Feuchtgruber, and M. Allen 2000b. Photochemistry of Saturn's atmosphere. II. Effects of an influx of external oxygen. *Icarus* **145**, 166–202.

Muhleman, D. O., G. L. Berge, and R. T. Clancy 1984. Microwave measurements of carbon monoxide on Titan. *Science* **223**, 393–396.

Noll, K. S., T. R. Geballe, R. F. Knacke, and Y. J. Pendleton 1996. Titan's 5 μm spectral window: Carbon monoxide and the albedo of the surface. *Icarus* **124**, 625–631.

Orton, G. S. 1992. In *Symposium on Titan*, ESA SP-338 (B. Kaldeich, Ed.), p. 81. European Space Agency, Noordwijk, The Netherlands.

Oser, H., N. D. Stothard, R. Humpfer, and H. H. Grotheer 1992. Direct measurement of the reaction $CH_3 + OH$ at ambient temperature in the pressure range 0.3–6.2 mbar. *J. Phys. Chem.* **96**, 5359–5363.

Owen, T., N. Biver, A. Marten, H. Matthews, and R. Meier 1999. *IAU Circ.* 7307.

Pepin, R. O. 1991. On the origin and early evolution of terrestrial planet atmospheres and meteoritic volatiles. *Icarus* **92**, 2–79.

Pereira, R. A., D. L. Baulch, M. J. Pilling, S. H. Robertson, and G. Zeng 1997. Temperature and pressure dependence of the multichannel rate coefficients for the $CH_3 + OH$ system. *J. Phys. Chem. A* **101**, 9681–9693.

Pinto, J. P., J. I. Lunine, S. J. Kim, and Y. L. Yung 1986. D to H ratio and the origin and evolution of Titan's atmosphere. *Nature* **319**, 388–390.

Röckmann, T., C. A. M. Brenninkmeijer, G. Saueressig, P. Bergamaschi, J. N. Crowley, H. Fischer, and P. J. Crutzen 1998. Mass-independent oxygen isotope fractionation in atmospheric CO as a result of the reaction CO + OH. *Science* **281**, 544–546.

Steinfeld, J. I., J. S. Francisco, and W. L. Hase 1989. *Chemical Kinetics and Dynamics*. pp. 248–250. Prentice-Hill, Englewood Cliffs, NJ.

Strobel, D. F. 1974. The photochemistry of hydrocarbons in the atmosphere of Titan. *Icarus* **21**, 466–470.

Van Dishoeck, E. F., G. A. Blake, B. T. Draine, and J. I. Lunine 1993. In *Protostars and Planets III*. (E. H. Levy and J. L. Lunine, Eds.), pp. 163–241. Univ. of Arizona Press, Tucson.

Yung, Y. L., M. Allen, and J. P. Pinto 1984. Photochemistry of the atmosphere of Titan: Comparison between model and observations. *Astrophys. J. Suppl.* **55**, 465–506.